

WARM AND COLD MONTHLY ANOMALIES ACROSS THE MEDITERRANEAN BASIN AND THEIR RELATIONSHIP WITH CIRCULATION; 1860–1990

PANAGIOTIS MAHERAS^{a,*}, ELENI XOPLAKI^{a,1}, TREVOR DAVIES^b, JAVIER MARTIN-VIDE^c,
MARIANO BARIENDOS^c and MARIA JÓAO ALCOFORADO^d

^a *Department of Meteorology and Climatology, University of Thessaloniki, Thessaloniki, GR-54006, Greece*

^b *Climatic Research Unit, School of Environmental Sciences, University of East Anglia, Norwich, NR4 7TJ, UK*

^c *Department of Physical Geography, University of Barcelona, Barcelona, 08028, Spain*

^d *Centre of Geographical Studies, University of Lisbon, Lisbon, 1699, Portugal*

Received 29 January 1998

Revised 9 March 1999

Accepted 16 March 1999

ABSTRACT

Anomalously warm and cold months in the Mediterranean basin were identified during the period 1860–1990 from observations at five stations located along the west–east axis of the Mediterranean basin (Barcelona, Florence, Malta, Athens and Jerusalem), supplemented by data from Madrid and Lisbon. Warm months were characterized by thermic indices (TI) based on values of the standardized anomalous temperatures. Different patterns of anomalously warm and cold months were qualitatively identified on the basis of the spatial distributions of the TIs. The standardized sea-level pressure (SLP) values at 56 grid points in the domain 35–65°N, 30°W–40°E, for each of the anomalously warm and cold months, were subjected to T-mode Principal Component Analysis. The mean TIs associated with each principal component in each season, for both warm and cold months, are arranged in four distinct different spatial distributions: (i) a Mediterranean-wide distribution of positive/negative anomalies; (ii) strong positive/negative anomalies in the west and central Mediterranean and weaker anomalies in the east; (iii) strong positive/negative anomalies in the eastern Mediterranean and weaker anomalies in central and western parts; (iv) strong positive/negative anomalies in the central Mediterranean and weaker anomalies in eastern and western parts. Finally, monthly mean charts of standardized anomaly and mean sea-level pressure charts are constructed for each principal component in each season, and are used to interpret the spatial distribution of the positive and negative temperature anomalies in terms of mean circulation over the domain. Copyright © 1999 Royal Meteorological Society.

KEY WORDS: temperature anomalies; Mediterranean; Principal Component Analysis; pressure pattern; atmospheric circulation

1. INTRODUCTION

The Mediterranean can be regarded as a transitional zone between the continental influences of Europe and Asia, the desert climate of North Africa and the oceanic effects from the Atlantic. The surface pressure field is influenced by the oceanic Azores High, the Siberian winter anticyclone, the northwestern extension of the South Asian summer thermal low, as well as more transient anticyclones and travelling depressions. The large longitudinal extent of the Mediterranean region, between 10°W and 35°E, is reflected in the Mediterranean Oscillation, a pressure seesaw between east and west, apparent not only at the surface (Maheras *et al.*, 1997) but also at 500 hPa (Conte *et al.*, 1989). The seesaw behaviour is also observed in other surface climatic variables (Maheras *et al.*, 1997). There are links with the pressure seesaw of the North Atlantic Oscillation (NAO) (Rogers, 1984; Moses *et al.*, 1987), with the low index NAO phase being associated with wet conditions in the western Mediterranean (Wanner *et al.*, 1995).

* Correspondence to: Department of Meteorology and Climatology, University of Thessaloniki, Thessaloniki, GR-54006, Greece. Tel.: +30 31 998471; fax: +30 31 995392; e-mail: maheras@geo.auth.gr

¹ Current address: Institute of Geography, University of Bern, Hallerstrasse 12, CH-3012, Bern, Switzerland

Orography is a significant influence, especially in the blocking and channelling of cold air masses. The northern coastline of the Mediterranean is jagged, and is surrounded by a chain of rather high mountains. It provides barriers against and openings toward air currents which bring extreme differences of air masses to play upon the region. As a consequence, sea–air heat exchange occurs, i.e. heating of the air flowing over the warmer sea and cooling of the sea by local katabatic winds like the Mistral in the Rhone Valley (Besleaga, 1991), the Bora in Adriatic sea and the Vardaris in the Thessaloniki valley (Maheras, 1982).

There have been a number of studies of the links between circulation patterns and surface climatic variables. Bartzokas and Metaxas (1991) established that recent trends in surface temperature across the Mediterranean region are as a result of changes in circulation. Kozukowski *et al.* (1992) explored the relationships between temperature and precipitation at stations in the Balkans and the height of the 500 hPa field. Metaxas and Bartzokas (1994) identified the ‘centres of action’ (quasi-permanent synoptic circulation, denoted by sea-level pressure (SLP) patterns which have pronounced effects on the climate in larger areas) which influenced temperature, precipitation and winds in Athens, whilst Corte-Real *et al.* (1995) related surface climatic variables over the whole Mediterranean area to circulation anomalies. Amongst the findings of Kutiel and Maheras (1998) and Maheras and Kutiel (1999), who examined the relationship between surface temperature and circulation indices, was the clear positive relationship of temperature with a high zonal index. Reddaway and Bigg (1996) extended the links between surface wind field and surface pressure to sea-surface temperature, and suggested links between the climate of the eastern Mediterranean and the South Asian monsoon.

The objective of this study is to take another step in this research, by establishing the relationship between mean monthly temperature anomalies in the Mediterranean area and the large-scale circulation over Europe, the Mediterranean and the near-Atlantic. These relationships were used, in a later study, to help interpret anomalous circulation patterns which have been reconstructed in the ‘early instrumental period’ (EIP) (1780–1860) (Xoplaki *et al.*, in press) and anomalous temperature patterns in the Late Maunder Minimum (LMM) period (1675–1715), both parts of the European Commission ADVICE research project.

2. DATA AND METHODS

Mean monthly temperature data were used for the period 1860–1990 from five stations aligned west–east along the main axis of the Mediterranean basin (Barcelona, Florence, Malta, Athens, Jerusalem), as well as from Lisbon and Madrid. All time series present a remarkable homogeneity (Kutiel and Maheras, 1998). The earliest date used is 1860 because earlier data are not available for the easternmost stations of Athens and Jerusalem. Gridded monthly SLP data at 5° and 10° latitude intervals have also been used in the domain 35–65°N, 30°W–40°E. The domain is similar to the one for which pressure reconstructions were made in the early instrumental period (1780–1860) in the European Commission ADVICE project (Jones *et al.*, 1999). For each station, standardized temperature anomalies for all months have been calculated using:

$$\text{sat} = (x - \bar{x})/\sigma$$

where \bar{x} is the long-term monthly mean temperature for each station, x is the mean temperature of a particular month and σ is the standard deviation. Thermic indices (TI) were constructed for each month in the 1860–1990 period according to the scheme in Table I.

Table I. Classification of sat into TIs

sat < -2.11	-2.1 < sat < -1.41	-1.4 < sat < -0.71	-0.7 < sat < 0.7	0.71 < sat < 1.4	1.41 < sat < 2.1	sat > 2.11
-3	-2	-1	0	+1	+2	+3

Table II. PCA–Varimax standardized explained variance of the principal components positive TIs

Season				
Winter				
Factor	1	2	3	4
Explained variance (%)	31.0	23.5	16.5	22.4
Cumulative explained variance (%)	31.0	54.5	71.0	93.4
Spring				
Factor	1	2	3	4
Explained variance (%)	36.1	22.6	23.6	9.0
Cumulative explained variance (%)	36.1	58.7	82.3	91.3
Summer				
Factor	1	2	3	4
Explained variance (%)	38.3	20.6	15.5	13.0
Cumulative explained variance (%)	38.3	58.9	74.4	87.4
Autumn				
Factor	1	2	3	
Explained variance (%)	51.8	21.3	13.9	
Cumulative explained variance (%)	51.8	73.1	87.0	

The scheme has been used to produce indices, which are similar to the TIs used in the LMM (Pfister *et al.*, 1994). For each station, warm months were defined as months with $TI = 2, 3$ and cold months had $TI = -2, -3$. At least three of the seven stations (using four stations the number of characteristic months, as warm or cold decrease considerably) had to conform to these definitions before a particular month was characterized as being anomalously warm or cold. The months were then assigned to the relevant seasons: winter (DJF); spring (MAM); summer (JJA); or autumn (SON).

For each of the anomalously warm and anomalously cold months, the standardized (by month) value of SLP was calculated for each of the 56 grid points. The resulting pressure patterns were then subjected to T-mode principal component analysis (PCA) with Varimax rotation (Richman, 1986), in order to establish those SLP patterns associated with the monthly temperature anomalies. Charts of the mean absolute SLP and standardized SLP anomalies from the months (in each of the four seasons) which had the greatest (positive or negative) loading on a particular significant principal component (either 3 PC or 4 PC, Tables II and IV) were constructed. In some cases, two sets of mean charts were constructed for each PC; (on the charts, for a better representation, the latitude is extended to 30°N) one for the greatest positive loading, and one for the greatest negative loading.

To aid the discussion of the results, the mean TI for each station is calculated from all the monthly TI values for the months associated with a particular set of charts.

Only the most frequent of particular spatial patterns of TI values in the anomalously warm or cold months (see below) are analysed here. The remaining cases were relatively infrequent and, moreover, were quite similar to the analysed cases.

3. RESULTS

3.1. Positive thermic index values

Winter: 21 months were identified. The PCA defined four significant components, which cumulatively explained 93.4% of the total variance (Table II). The selection of the components has been undertaken according to the Kaiser (1959) rule. The first principal component (PC1) includes 7 months with positive loadings (Table III); PC2 includes 4 months with positive loadings and 3 months with negative loadings; PC3 includes 3 months with positive loadings; PC4 includes 4 months with positive loadings.

Table III. Mean TIs for the principal components for positive and negative loading values positive TIs

Winter	Lisbon	Madrid	Barcelona	Florence	Malta	Athens	Jerusalem
Factor 1+ (7)	1.7	1.6	1.3	1.3	1.6	1.7	1.6
Factor 2+ (4)	2.5	2.5	2.0	1.0	1.3	1.0	1.0
Factor 3+ (3)	2.0	1.7	1.3	1.7	1.0	1.7	0.3
Factor 4+ (4)	1.5	1.3	2.3	2.5	1.5	1.8	0.8
Factor 2- (3)	2.3	2.0	1.7	2.0	1.3	0.7	-0.3
Spring							
Factor 1+ (7)	2.3	2.1	1.7	1.3	1.0	0.7	-0.6
Factor 2+ (5)	-0.4	-0.2	1.0	1.4	2.2	2.6	1.2
Factor 3+ (5)	0.8	2.0	1.8	1.8	1.4	0.2	-0.6
Factor 4+ (1)	2.0	2.0	2.0	1.0	0.0	0.0	-1.0
Summer							
Factor 1+ (8)	1.4	2.0	1.9	1.6	1.5	0.1	-0.4
Factor 2+ (2)	0.5	-0.5	2.0	2.0	2.0	0.0	0.0
Factor 3+ (3)	0.0	1.0	1.3	1.0	1.7	1.3	1.7
Factor 1- (1)	0.0	-1.0	0.0	1.0	2.0	2.0	2.0
Factor 2- (2)	0.0	2.0	0.5	-1.0	1.5	1.0	2.5
Factor 4- (1)	1.0	1.0	2.0	2.0	1.0	2.0	0.0
Autumn							
Factor 1+ (7)	2.4	2.3	2.0	0.7	0.6	-0.4	-0.4
Factor 2+ (2)	1.0	0.0	0.5	0.0	2.0	1.5	1.5
Factor 3+ (2)	1.5	1.5	1.5	1.5	1.0	1.0	0.5
Factor 1- (2)	-1.0	-0.5	0.0	1.0	0.5	3.0	1.5
Factor 2- (1)	2.0	2.0	2.0	0.0	0.0	0.0	0.0

+ : Positive loading; - : negative loading; () : number of cases-months used in each case to produce the plots in Figures 1-10.

Spring: 18 months were identified. Four significant components explained 91.3% of the total variance. PC1 includes 7 months with positive loadings (Table III); PC2 includes 5 months with positive loadings; PC3 includes 5 months with positive loadings; PC4 includes 1 month with a positive loading.

Summer: 17 months were identified. Again, four significant components explained 87.4% of the total variance. PC1 includes 8 months with positive loadings and 1 month with negative loading (Table III); PC2 includes 2 months with positive loadings and 2 months with negative loadings; PC3 includes 3 months with positive loadings; PC4 includes 1 month with a negative loading.

Autumn: 14 months were identified. Three significant components explained 87% of the total variance. PC1 includes 7 months with positive loadings and 2 months with negative loadings (Table III); PC2 includes 2 months with positive loadings and 1 month with a negative loading; PC3 included 2 months with positive loadings.

The TI values associated with the PCs in Table III may be used to qualitatively group the positive temperature anomalies into a number of general patterns (Sections 3.1.1-3.1.4 below).

3.1.1. Almost uniform distribution of positive temperature anomalies over the whole Mediterranean. This distribution is most noticeable in winter (Table III; PC1, positive loading), with TI station values 1.3-1.7. It is not apparent in spring and summer, whilst it appears, but not often, during autumn (PC3, positive loading). Kutiel *et al.* (1996) linked such Mediterranean-wide warm winter conditions with greater zonality.

Figure 1 shows the mean standardized SLP anomaly pattern (Figure 1(a)) and the mean absolute SLP pattern (Figure 1(b)) for the winter season PC1. There is a strong negative pressure anomaly centred to the west of Iberia, which extends over most of the domain. This is associated with a SLP field, with a low to the west of the British Isles, with SW flow extending deep into the Mediterranean and a strong southerly component in the eastern part of the basin, reflecting basin-wide warm air advection.

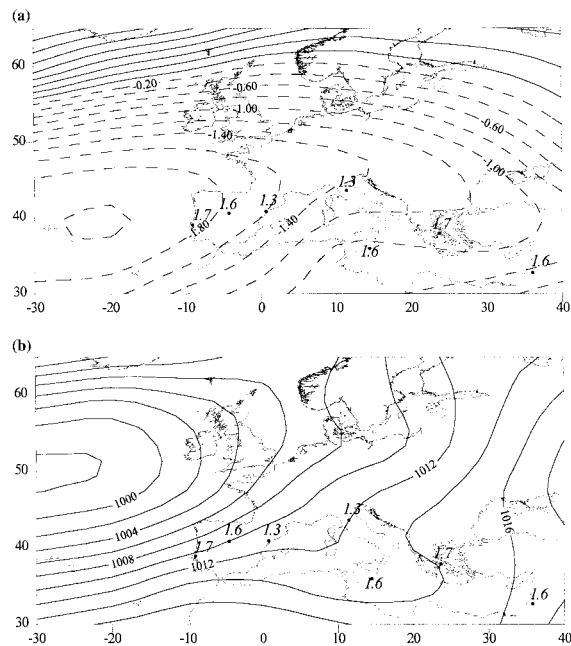


Figure 1. (a) Winter, PC1, positive loading values, mean standardized pressure values. The station values are the TIs for (from west to east) Lisbon, Madrid, Barcelona, Florence, Malta, Athens and Jerusalem. (b) Winter, PC1, positive loading values, mean sea-surface pressure values. The station values are the TIs for (from west to east) Lisbon, Madrid, Barcelona, Florence, Malta, Athens and Jerusalem

Figure 2 shows the SLP anomaly and SLP charts associated with the autumn PC3, positive loading. Figure 2(a) shows an anomalously strong zonal flow, especially over the western Mediterranean, and an extension of the Azores High into the eastern Mediterranean (see also Figure 2(b)). The TI values are greatest in the west of the Mediterranean, and diminish to the east, illustrating the importance of warm air advection from the Atlantic in autumn, which is less influential in the east because of the greater northerly component to the flow (Figure 2).

3.1.2. Strong positive anomalies to the west, but weaker to the east. This distribution appears in all seasons, but is most pronounced in spring (PC1, positive loading) and autumn (PC1, positive loading) (Table III). It also appears in winter (PC2, negative loading).

Figure 3(a) shows a strong positive SLP anomaly over the whole of the Mediterranean and southern Europe, extending up to about 50°N associated with the spring PC1 (positive loading). A ridge from the Azores High is the dominant feature (Figure 3(b)). The eastern Mediterranean experiences a northerly flow component, which, in spring, will lead to cooler conditions (e.g. the TI value at Jerusalem is -0.6), whereas the westerly flow, combined with anticyclonic conditions over Iberia leads to TI values 2.3 and 2.1 at Lisbon and Madrid, respectively (Figure 3(b)).

Figure 4 shows the charts for the autumn PC1, positive loading. A positive SLP anomaly is located over the central Mediterranean/Balkan area, but spreads over most of Europe (Figure 4(a)). Together with the negative anomaly in the Atlantic, this leads to pronounced southerly–southwesterly flow over the western Mediterranean (TI values 2.0–2.4 in Iberia; Figure 4). The eastern Mediterranean is affected by flow from the northeast, resulting in TI values -0.4 for Athens and Jerusalem.

The SLP distributions for the winter PC2, negative loading, display a negative anomaly to the west of the British Isles and a positive anomaly at the eastern edge of the domain (Figure 5(a)), reflecting vigorous zonal flow influencing Iberia (TI values 2.3 and 2.0 at Lisbon and Barcelona, respectively), a slack pressure field in the central Mediterranean and a Siberian influence in the east (TI value of -0.3 at Jerusalem).

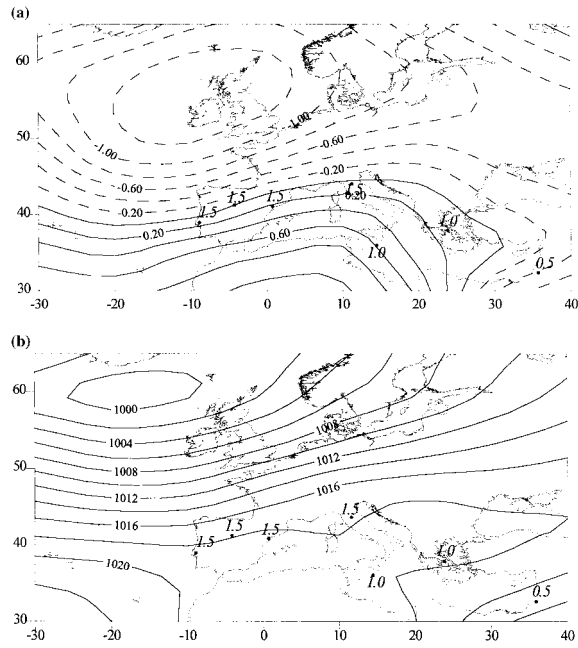


Figure 2. (a) Autumn, PC3, positive loading values, mean standardized pressure values. The station values are the TIs for (from west to east) Lisbon, Madrid, Barcelona, Florence, Malta, Athens and Jerusalem. (b) Autumn, PC3, positive loading values, mean sea-surface pressure values. The station values are the TIs for (from west to east) Lisbon, Madrid, Barcelona, Florence, Malta, Athens and Jerusalem

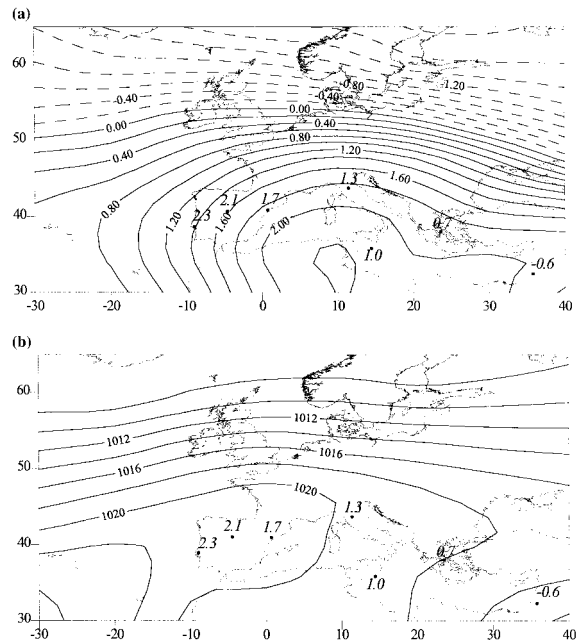


Figure 3. (a) Spring, PC1, positive loading values, mean standardized pressure values. The station values are the TIs for (from west to east) Lisbon, Madrid, Barcelona, Florence, Malta, Athens and Jerusalem. (b) Spring, PC1, positive loading values, mean sea-surface pressure values. The station values are the TIs for (from west to east) Lisbon, Madrid, Barcelona, Florence, Malta, Athens and Jerusalem

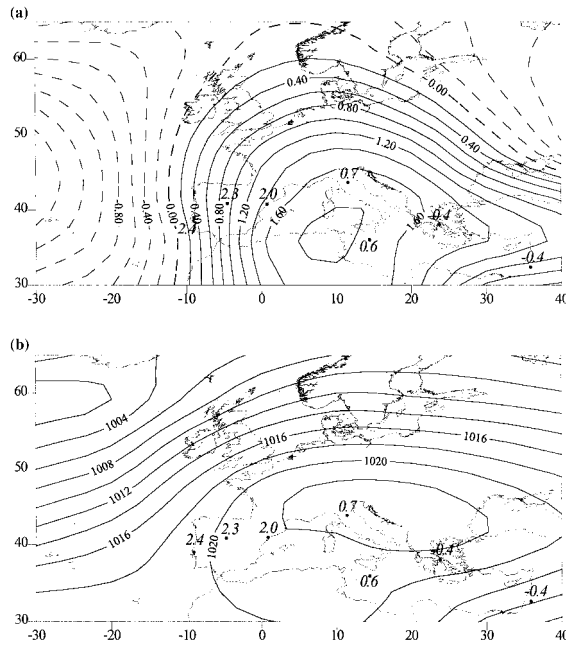


Figure 4. (a) Autumn, PC1, positive loading values, mean standardized pressure values. The station values are the TIs for (from west to east) Lisbon, Madrid, Barcelona, Florence, Malta, Athens and Jerusalem. (b) Autumn, PC1, positive loading values, mean sea-surface pressure values. The station values are the TIs for (from west to east) Lisbon, Madrid, Barcelona, Florence, Malta, Athens and Jerusalem

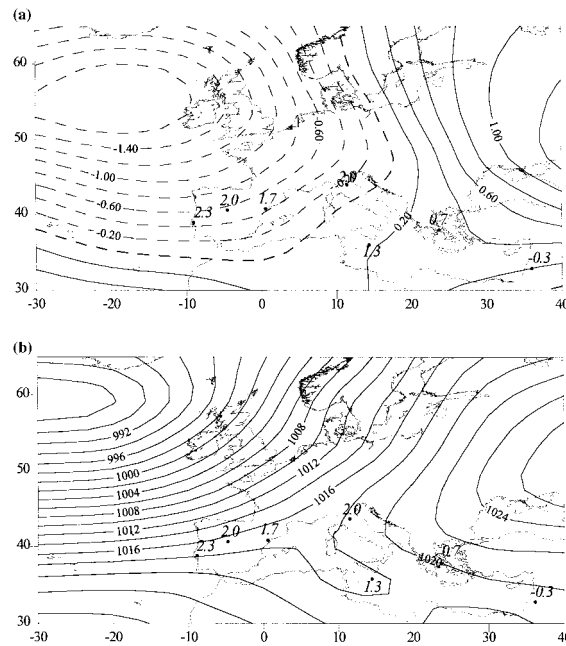


Figure 5. (a) Winter, PC2, negative loading values, mean standardized pressure values. The station values are the TIs for (from west to east) Lisbon, Madrid, Barcelona, Florence, Malta, Athens and Jerusalem. (b) Winter, PC2, negative loading values, mean sea-surface pressure values. The station values are the TIs for (from west to east) Lisbon, Madrid, Barcelona, Florence, Malta, Athens and Jerusalem

3.1.3. Strong positive anomalies to the east, and weaker ones to the west. This distribution appears in all seasons, albeit with a lower frequency than the previous distribution, and except for winter. Examples are spring PC2 (positive loading), summer PC3 (positive loading) and autumn PC1 (negative loading) (Table III).

In spring, for PC2 (positive loading), the SLP anomaly chart (Figure 6(a)) exhibits a negative zone to the west of the Bay of Biscay and affecting the western Mediterranean, to be replaced by a positive anomaly in the eastern extremity of the basin. The southerly position of the low to the west of the British Isles (Figure 6(b)), leads to pronounced westerly flow over Iberia, originating from higher, colder, oceanic latitudes on the eastern flank of the low. This is reflected in TI values -0.4 and -0.2 at Lisbon and Madrid, respectively. Further east, over the Mediterranean, the flow is southwesterly, leading to warmer conditions (e.g. TI values 2.2 and 2.6 at Malta and Athens, respectively).

For the summer PC3, positive loading, the SLP anomaly pattern (Figure 7(a)) is complex. There is a strong negative anomaly well to the west of the Straits of Gibraltar, a weaker one over the Baltic and a strong positive anomaly over the Middle East. The weakening of the Azores High to the west of Iberia, and the strong isobaric curvature over the peninsula leading to local north–northwesterly flow (Figure 7(b)), led to average and slightly warmer conditions (TI values 0.0–1.3 over Iberia). This case is an example of how, on occasions, it may be difficult to interpret monthly mean pressure charts. The explanation for the high TI values for Malta, Athens and Jerusalem is not obvious from the mean charts. However, examination of the daily charts indicated that a warm ridge, which extended for several days, from Libya, across Greece and Turkey, to the Black Sea (Figure 7(a)), led to frequent advection of warm air from the Sahara northwards and eastwards in the eastern part of the Mediterranean basin, and resulted in light northerly winds over the Aegean. This explanation is in agreement with Giles and Balafoutis (1990).

Figure 8 shows the charts for the autumn PC1 (negative loading) (compare with the relevant charts for the positive loading; Figure 4). An extensive negative SLP anomaly is centred on central Europe (Figure 8(a)) countered by a positive anomaly towards the western edge of the domain. The anomaly field reflects

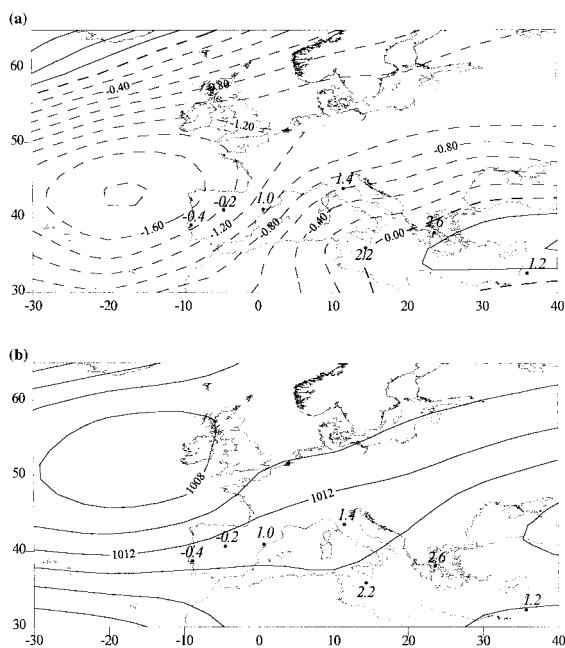


Figure 6. (a) Spring, PC2, positive loading values, mean standardized pressure values. The station values are the TIs for (from west to east) Lisbon, Madrid, Barcelona, Florence, Malta, Athens and Jerusalem. (b) Spring, PC2, positive loading values, mean sea-surface pressure values. The station values are the TIs for (from west to east) Lisbon, Madrid, Barcelona, Florence, Malta, Athens and Jerusalem

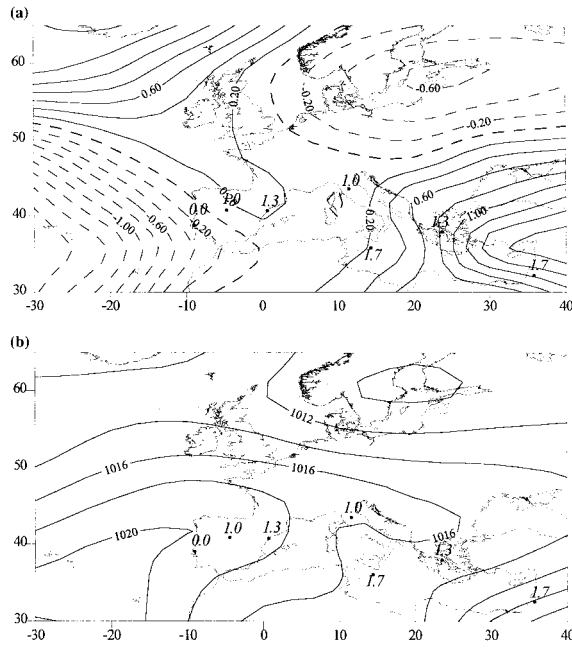


Figure 7. (a) Summer, PC3, positive loading values, mean standardized pressure values. The station values are the TIs for (from west to east) Lisbon, Madrid, Barcelona, Florence, Malta, Athens and Jerusalem. (b) Summer, PC3, positive loading values, mean sea-surface pressure values. The station values are the TIs for (from west to east) Lisbon, Madrid, Barcelona, Florence, Malta, Athens and Jerusalem

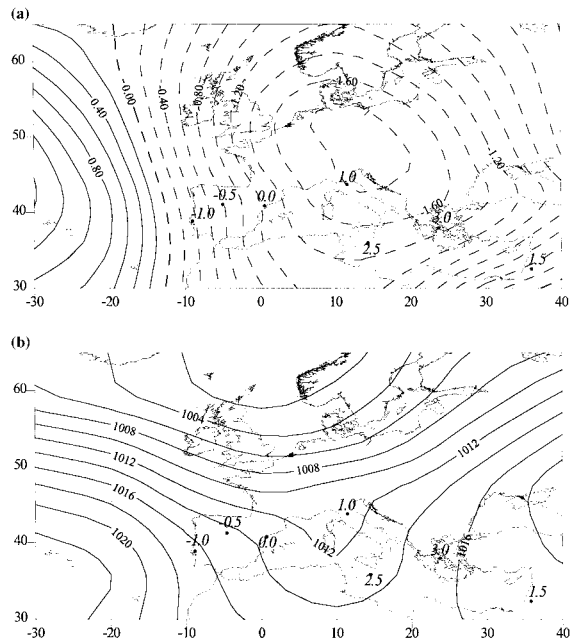


Figure 8. (a) Autumn, PC1, negative loading values, mean standardized pressure values. The station values are the TIs for (from west to east) Lisbon, Madrid, Barcelona, Florence, Malta, Athens and Jerusalem. (b) Autumn, PC1, negative loading values, mean sea-surface pressure values. The station values are the TIs for (from west to east) Lisbon, Madrid, Barcelona, Florence, Malta, Athens and Jerusalem

a pronounced trough with its axis to the west of Italy (Figure 8(b)), which produces the simply explained cooler conditions in the west (TI values 0.0 to -1.0 in Iberia) and warmer weather in the east (TI values 1.5 at Jerusalem, 2.5 at Malta and 3.0 in Athens).

3.1.4. Strong positive anomalies in the central Mediterranean. This distribution is most apparent in spring (PC3, positive loading) and summer (PC2, positive loading; Table III).

For the spring PC3 (positive loading) case, a positive SLP anomaly is centred on the Balkan region (Figure 9(a)), but extends over much of mainland Europe, giving way to a negative anomaly towards the northwest of the domain. The SLP field (Figure 9(b)) displays a narrow zone of high pressure, with very slack gradients, protruding from the Azores High towards the central Mediterranean; the settled conditions probably allowing high surface temperatures to develop, extending to the inland plateau location of Madrid, where the TI value was comparable with those in the central area (Barcelona, 1.8; Florence, 1.8; Malta, 1.4). On the other hand, the northeast flow in the east produced a TI value of -0.6 at Jerusalem.

For PC2 (positive loading) in summer, there was a distinct positive SLP anomaly over the British Isles/North Sea region and weak negative anomalies in the western and extreme eastern, Mediterranean (Figure 10(a)). The SLP field displays a broad ridge built up across west–central Europe, extending from the Azores High (Figure 10(b)). The regional flow to the central Mediterranean is from the northeast, so it seems likely that the slack pressure gradients allowed the development of a warm episode in this region, augmented by warm air advection from central Europe. Madrid and Lisbon, on the other hand (TI values -0.5 and 0.5 , respectively), were influenced by northeast flow from the Bay of Biscay. The pressure gradient over the eastern Mediterranean was strong (Figure 10(b)), with northeasterly flow around the low pressure producing average conditions at Athens and Jerusalem (TI value 0.0).

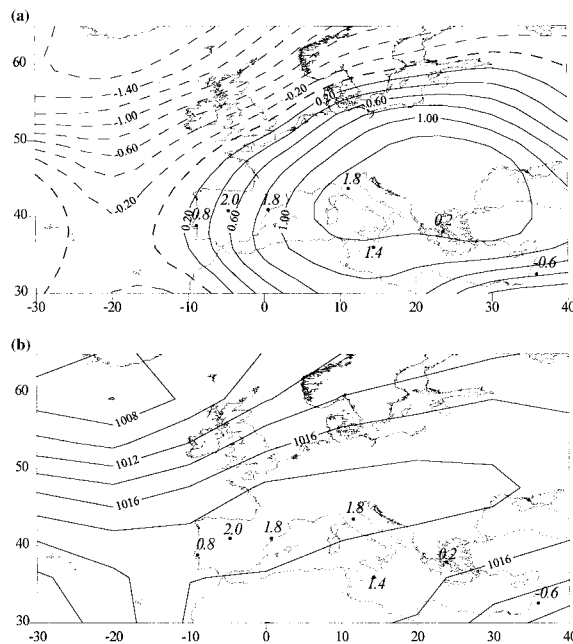


Figure 9. (a) Spring, PC3, positive loading values, mean standardized pressure values. The station values are the TIs for (from west to east) Lisbon, Madrid, Barcelona, Florence, Malta, Athens and Jerusalem. (b) Spring, PC3, positive loading values, mean sea-surface pressure values. The station values are the TIs for (from west to east) Lisbon, Madrid, Barcelona, Florence, Malta, Athens and Jerusalem

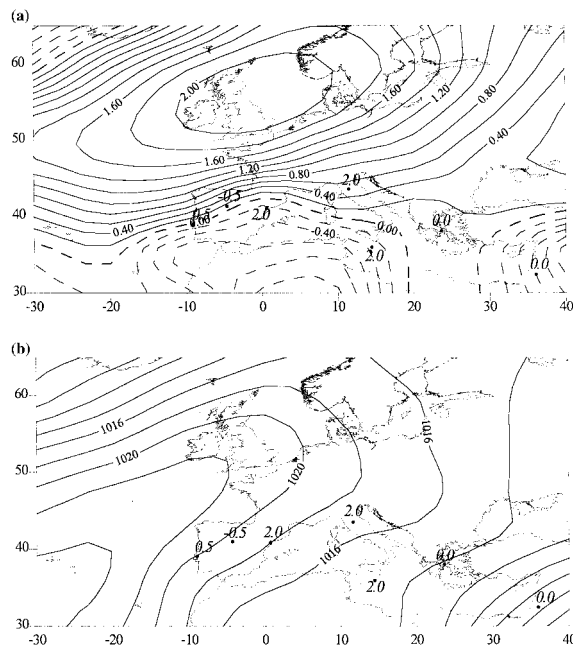


Figure 10. (a) Summer, PC2, positive loading values, mean standardized pressure values. The station values are the TIs for (from west to east) Lisbon, Madrid, Barcelona, Florence, Malta, Athens and Jerusalem. (b) Summer, PC2, positive loading values, mean sea-surface pressure values. The station values are the TIs for (from west to east) Lisbon, Madrid, Barcelona, Florence, Malta, Athens and Jerusalem

3.2. Negative thermic index values

Winter: 19 months were identified. The first four principal components cumulatively explained 95.4% of the total variance (Table IV). PC1 includes 6 months with positive loadings (Table V); PC2 includes 6 months with positive loadings and 2 months with negative loadings; PC3 includes 3 months with positive loadings; PC4 includes 2 months with positive loadings.

Table IV. PCA–Varimax standardized explained variance of the principal components negative TIs

Season				
Winter				
Factor	1	2	3	4
Explained variance (%)	30.1	30.0	19.4	15.9
Cumulative explained variance (%)	30.1	60.1	79.5	95.4
Spring				
Factor	1	2	3	4
Explained variance (%)	27.8	26.3	24.5	12.2
Cumulative explained variance (%)	27.8	54.1	78.6	90.8
Summer				
Factor	1	2	3	
Explained variance (%)	32.1	26.7	25.1	
Cumulative explained variance (%)	32.1	58.7	83.8	
Autumn				
Factor	1	2	3	
Explained variance (%)	41.8	22.1	19.8	
Cumulative explained variance (%)	41.8	63.9	83.7	

Table V. Mean TIs for the principal components for positive and negative loading values negative TIs

Winter	Lisbon	Madrid	Barcelona	Florence	Malta	Athens	Jerusalem
Factor 1+ (6)	-2.0	-1.8	-1.8	-2.7	-1.0	-1.2	0.0
Factor 2+ (6)	-1.2	-1.2	-2.2	-2.2	-1.5	-2.2	-1.0
Factor 3+ (3)	-1.0	-1.7	-2.0	-1.7	-2.0	-1.0	0.3
Factor 4+ (2)	-2.0	-3.0	-2.5	-2.5	-2.0	-1.0	0.5
Factor 2- (2)	-2.5	-3.0	-1.0	-2.0	-2.0	0.0	0.0
Spring							
Factor 1+ (6)	-1.7	-2.0	-1.8	-1.3	-1.3	0.0	1.0
Factor 2+ (2)	-2.0	-2.5	-1.5	-0.5	0.0	1.0	0.0
Factor 3+ (5)	-1.6	-2.0	-2.2	-1.8	-0.4	0.0	1.0
Factor 4+ (2)	1.0	0.5	-0.5	-2.0	-1.5	-2.5	-2.0
Factor 1- (1)	0.0	0.0	0.0	-1.0	-2.0	-2.0	-2.0
Factor 2- (1)	0.0	0.0	-1.0	-2.0	3.0	-3.0	-3.0
Summer							
Factor 1+ (6)	-0.5	-1.7	-1.5	-2.0	-1.3	-1.0	0.7
Factor 2+ (3)	-1.3	-1.7	-1.3	-1.3	-1.3	-1.3	-0.3
Factor 3+ (4)	-0.8	-1.8	-1.3	-0.5	-1.5	-0.8	-0.5
Factor 2- (1)	2.0	0.0	0.0	-1.0	-2.0	-2.0	-2.0
Autumn							
Factor 1+ (6)	-1.0	-1.8	-2.5	-2.3	-1.0	-0.2	0.3
Factor 2+ (1)	0.0	0.0	0.0	-2.0	-2.0	-2.0	0.0
Factor 3+ (1)	-3.0	-3.0	-2.0	0.0	0.0	2.0	2.0
Factor 2- (2)	-2.0	-2.0	-2.5	-1.5	0.0	1.0	1.0
Factor 3- (1)	0.0	0.0	-2.0	-2.0	-3.0	0.0	0.0

+ : Positive loading; - : negative loading; () : number of cases-months used in each case to produce the plots in Figures 1-10.

Spring: 17 months were identified. Four principal components explain 90.8% of the total variance (Table IV). PC1 includes 6 months with positive loadings and 1 month with a negative loading (Table V); PC2 includes 2 months with positive loadings and one with a negative loading; PC3 includes 5 months with positive loadings; PC4 includes 2 months with positive loadings.

Summer: 14 months were identified. Three significant principal components explain 83.8% of the total variance (Table IV). PC1 includes 6 months with positive loadings (Table V); PC2 includes 3 months with positive loadings and 1 month with a negative loading; PC3 includes 4 months with positive loadings.

Autumn: 11 months were identified. Three significant principal components explain 83.7% of the total variance (Table IV). PC1 includes 6 months with positive loadings (Table V); PC2 includes 1 month with a positive loading and 2 months with negative loading; PC3 includes 1 month with a positive loading and 1 month with a negative loading.

The TI values associated with the PCs in Table V are used to qualitatively group the negative temperature anomalies into a number of general patterns across the Mediterranean, in a similar fashion as for the positive TI values, discussed above. Again, four general patterns were identified (as Sections 3.2.1-3.2.4 below).

3.2.1. Almost uniform distribution of negative temperature anomalies over the whole Mediterranean.. This distribution is most frequent in winter (Table V; PC1 and PC2, positive loadings), but also in summer (PC2, positive loading). The following two examples from winter are used to illustrate the links with the circulation.

For PC1 (positive loading), there is a positive SLP anomaly to the northwest of the British Isles (Figure 11(a)), and the SLP field is centred on a high pressure over the English Channel (Figure 11(b)). This leads to flow over most of the Mediterranean from continental Europe or Asia, thus leading to the low TI

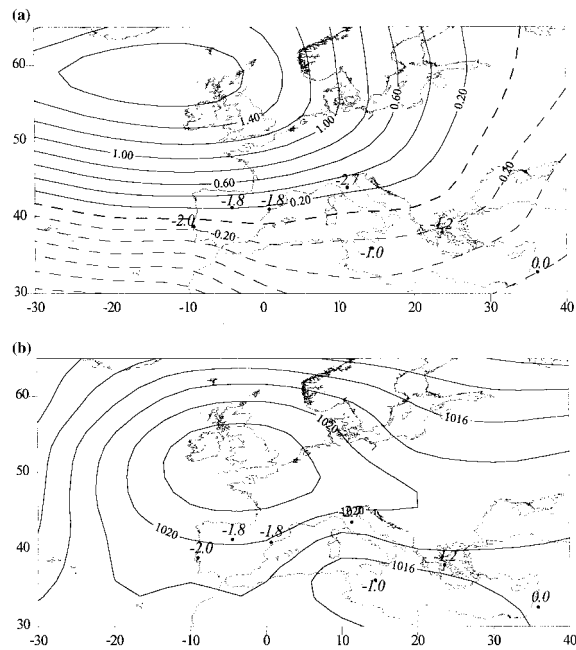


Figure 11. (a) Winter, PC1, positive loading values, mean standardized pressure values. The station values are the TIs for (from west to east) Lisbon, Madrid, Barcelona, Florence, Malta, Athens and Jerusalem. (b) Winter, PC1, positive loading values, mean sea-surface pressure values. The station values are the TIs for (from west to east) Lisbon, Madrid, Barcelona, Florence, Malta, Athens and Jerusalem

values (-1.2 to -2.7) everywhere except Jerusalem (TI value of 0.0), where the flow has a southerly component.

There is also a positive SLP anomaly apparent in the PC2 (positive loading) charts, but this time it is centred over eastern Europe (Figure 12(a)), reflecting a longitudinally extensive high over the northern margins of the Mediterranean (Figure 12(b)). This time, the eastern Mediterranean is also under the influence of cold outflow from Asia (TI value of -1.0 at Jerusalem), and the continuing easterly flow over the entire basin produces TI values between -1.2 and -2.2 .

3.2.2. Strong negative anomalies to the west, but weaker or positive to the east. This distribution is more frequent during spring (PC1, positive loading) and autumn (PC1, positive loading), but can appear throughout the year (e.g. in winter, PC3, positive loading (Table V)).

For the spring PC1 (positive loading), there is a distinct negative SLP anomaly over central regions of the Mediterranean (Figure 13(a)), which influences most of Europe. The SLP field mirrors the anomaly field, with the low over Italy (Figure 13(b)) being associated with cold air invasions from the north into west-central Mediterranean (TI values between -1.3 and -2.0), whereas eastern parts of the basin are beyond their direct influence (TI values 0.0 and 1.0 at Athens and Jerusalem, respectively).

For autumn PC1 (positive loading), there is a positive SLP anomaly to the west of the British Isles, balanced by a weaker negative anomaly over the Black Sea/Turkey region (Figure 14(a)). The SLP field reveals a closed high over northern Iberia, France and southern British Isles, extending westwards into the Atlantic (Figure 14(b)). This induces cold continental air from the continent into the west-central Mediterranean (TI values between -1.0 and -2.5), whereas temperatures in the east are more normal (TI values -0.2 and 0.3 at Athens and Jerusalem, respectively).

For the winter PC3 (positive loading) case, there is a broad zone of negative SLP anomaly over the Mediterranean region, and a positive anomaly towards the northeast of the domain (Figure 15(a)). The SLP field displays the Siberian anticyclone ridging out towards northwest Europe and southern Scandinavia, whilst the low over the central Mediterranean will entrain some of the cold continental air into

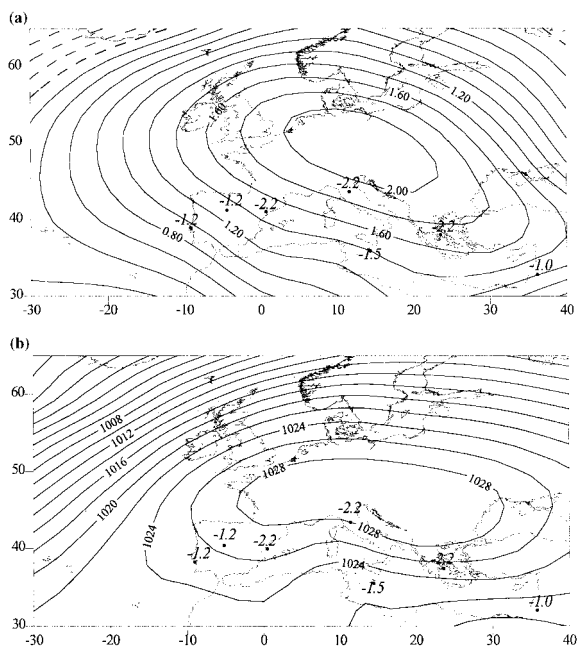


Figure 12. (a) Winter, PC2, positive loading values, mean standardized pressure values. The station values are the TIs for (from west to east) Lisbon, Madrid, Barcelona, Florence, Malta, Athens and Jerusalem. (b) Winter, PC2, positive loading values, mean sea-surface pressure values. The station values are the TIs for (from west to east) Lisbon, Madrid, Barcelona, Florence, Malta, Athens and Jerusalem

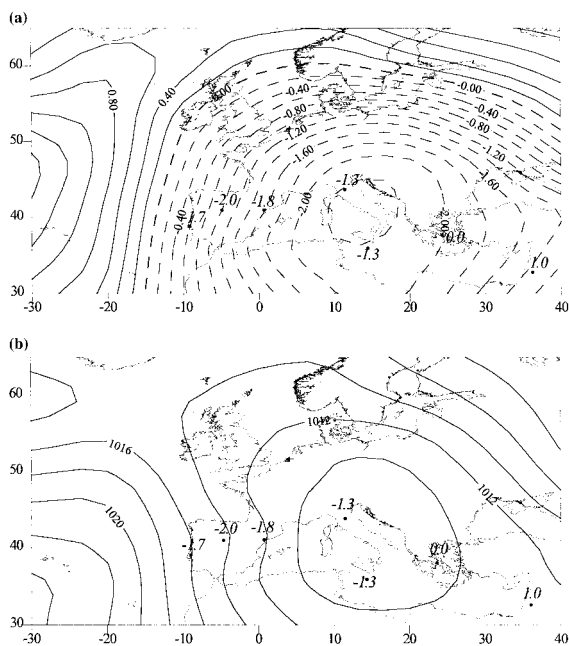


Figure 13. (a) Spring, PC1, positive loading values, mean standardized pressure values. The station values are the TIs for (from west to east) Lisbon, Madrid, Barcelona, Florence, Malta, Athens and Jerusalem. (b) Spring, PC1, positive loading values, mean sea-surface pressure values. The station values are the TIs for (from west to east) Lisbon, Madrid, Barcelona, Florence, Malta, Athens and Jerusalem

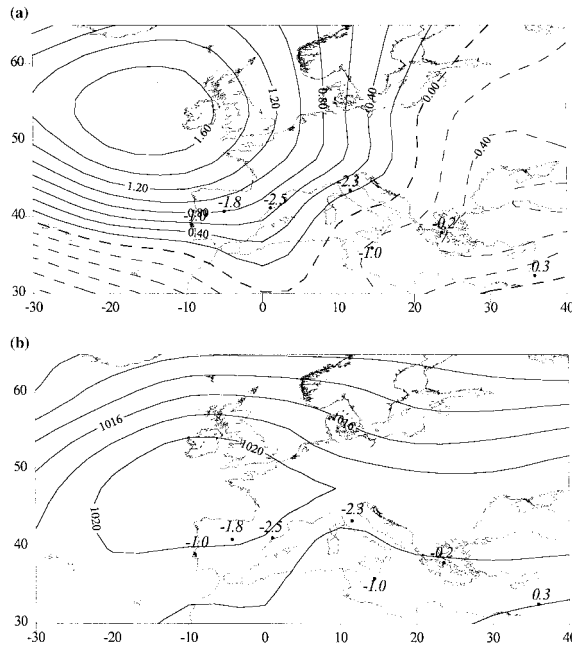


Figure 14. (a) Autumn, PC1, positive loading values, mean standardized pressure values. The station values are the TIs for (from west to east) Lisbon, Madrid, Barcelona, Florence, Malta, Athens and Jerusalem. (b) Autumn, PC1, positive loading values, mean sea-surface pressure values. The station values are the TIs for (from west to east) Lisbon, Madrid, Barcelona, Florence, Malta, Athens and Jerusalem

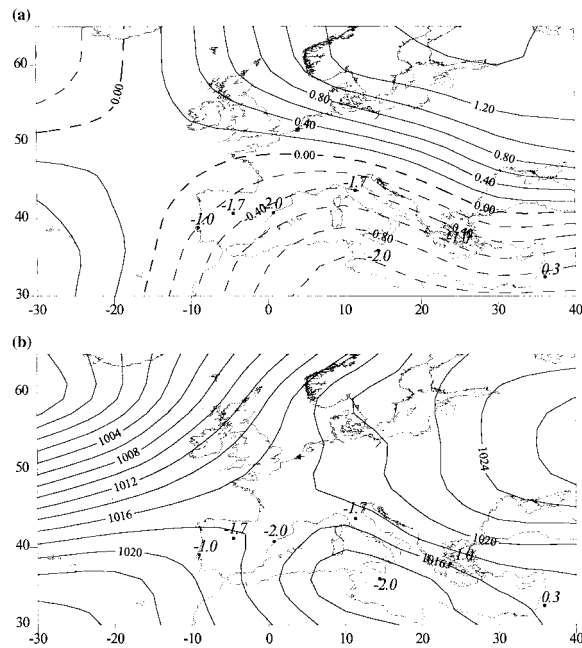


Figure 15. (a) Winter, PC3, positive loading values, mean standardized pressure values. The station values are the TIs for (from west to east) Lisbon, Madrid, Barcelona, Florence, Malta, Athens and Jerusalem. (b) Winter, PC3, positive loading values, mean sea-surface pressure values. The station values are the TIs for (from west to east) Lisbon, Madrid, Barcelona, Florence, Malta, Athens and Jerusalem

western and central parts of the basin (Figure 15(b)). The resulting TI values are between -1.7 and -2.0 , whilst even Athens has a value of -1.0 , because of the Asian influence, although the flow from the southeast at the easternmost margins leads to a near-normal TI value at Jerusalem.

3.2.3. Strong negative anomalies to the east, but weaker or positive ones to the west. Summer and spring are the seasons during which this is a relatively frequent distribution; for example, PC4 (positive loading) in spring and PC2 (negative loading) in summer (Table V).

There is a broad positive anomaly in the SLP field for spring PC4 (positive loading), stretching from the Baltic to beyond the English Channel (Figure 16(a)). This reflects a long extension of the Siberian High to link with the Azores High (Figure 16(b)), with a deeper-than-normal low over the eastern Mediterranean (Figure 16(a)). The outflow of cold Siberian air affects eastern and central parts of the Mediterranean (TI values -1.5 to -2.5), whilst the westernmost extremity (TI value of 1.0 at Lisbon) is probably influenced by southwesterly flow from the tropical Atlantic.

The charts for summer PC2 (negative loading) indicate higher-than-normal SLP over most of Europe, spreading from the southwest of the domain (Figure 17(a)). Synoptic experience suggests that the reason for the cold condition in the eastern Mediterranean (TI values -2.0 at Malta, Athens and Jerusalem) is the incursion air behind cold fronts as depressions are steered around the northern flank of the ridge (Maheras, 1982).

3.2.4. Strong negative anomalies in the central Mediterranean. Although this type of distribution occurs in one month only, in autumn PC3 (negative loading), it is such a distinctive pattern (TI values -2.0 at Barcelona and Florence and -3.0 at Malta; with values 0.0 at all other stations) (Table V) that it will be considered here. Another reason for consideration is that it also produces a distinctive SLP anomaly pattern, with a strongly positive zone over the central Mediterranean region, extending to most other parts of Europe (Figure 18(a)). The SLP field displays a weak high over central Europe, with a col through to the Azores High (Figure 18(b)). The low TI values in the central Mediterranean may be a result of the northeasterly flow out of eastern Europe as the land surface cools in autumn.

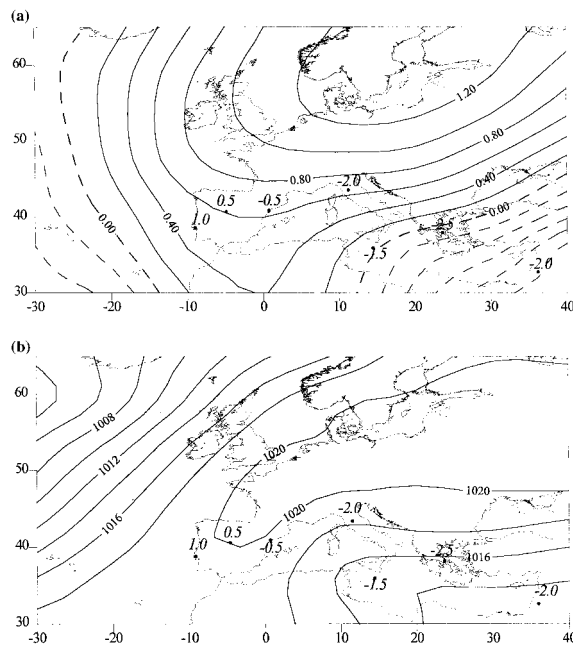


Figure 16. (a) Spring, PC4, positive loading values, mean standardized pressure values. The station values are the TIs for (from west to east) Lisbon, Madrid, Barcelona, Florence, Malta, Athens and Jerusalem. (b) Spring, PC4, positive loading values, mean sea-surface pressure values. The station values are the TIs for (from west to east) Lisbon, Madrid, Barcelona, Florence, Malta, Athens and Jerusalem

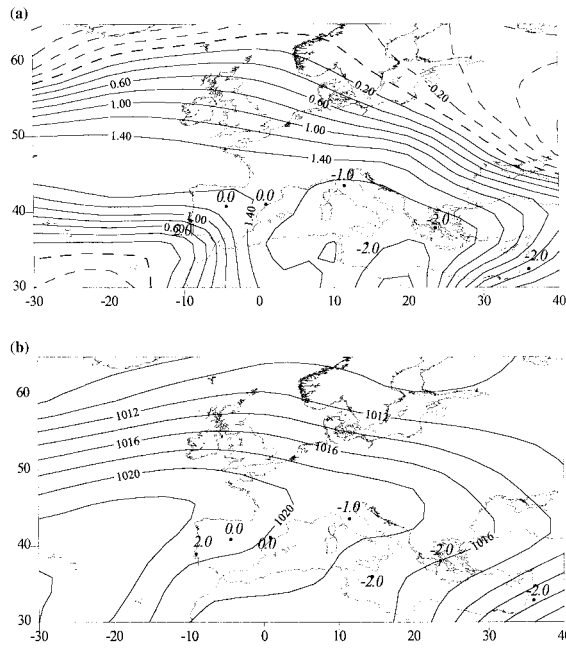


Figure 17. (a) Summer, PC2, negative loading values, mean standardized pressure values. The station values are the TIs for (from west to east) Lisbon, Madrid, Barcelona, Florence, Malta, Athens and Jerusalem. (b) Summer, PC2, negative loading values, mean sea-surface pressure values. The station values are the TIs for (from west to east) Lisbon, Madrid, Barcelona, Florence, Malta, Athens and Jerusalem

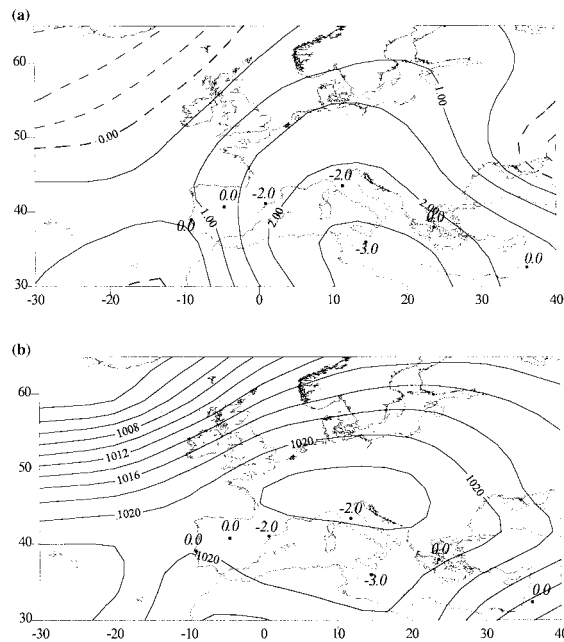


Figure 18. (a) Autumn, PC3, negative loading values, mean standardized pressure values. The station values are the TIs for (from west to east) Lisbon, Madrid, Barcelona, Florence, Malta, Athens and Jerusalem. (b) Autumn, PC3, negative loading values, mean sea-surface pressure values. The station values are the TIs for (from west to east) Lisbon, Madrid, Barcelona, Florence, Malta, Athens and Jerusalem

4. CONCLUSIONS

Winter is the season with the greatest frequency of months of temperature anomalies over the Mediterranean (21 warm, 19 cold). Autumn has the smallest number of cases of cold months (11) and summer the smallest number of warm months (13). The variance in the monthly pressure fields related to the temperature anomalies explained by the significant principal components is also greatest for winter (95.3% for the cold months, 93.4% for the warm months). Such relative clarity of, and coherency in, behaviour in winter has been remarked upon by other researchers (Maheras, 1989; Maheras and Kolyva-Machera, 1993; Rossetti and Maheras, 1995), and can be directly related to the average strong zonality of flow, and departures therefrom. The transition season of autumn exhibits the lowest level of explanation in the PCA (83.7 and 87% for the cold and warm months, respectively).

The PCA was largely successful in isolating the main pressure distributions over the study domain, which are associated with (qualitatively identified) monthly temperature anomaly patterns, and so was a considerable aid in interpreting the occurrence and character of the warm and cold months. By and large, winter is the season in which the character of the warm and cold months can most easily be interpreted in terms of circulation patterns. Summer is the most problematical of the seasons to interpret, because there is relatively weak discrimination between the mean monthly charts as a result of the strong persistence of anticyclonic conditions over the Atlantic and Europe and the pronounced stability of the thermal low over the eastern Mediterranean. In spring and autumn, meridional circulation is at its highest frequency (Maheras, 1982). During these seasons, the phenomenon of the Mediterranean Oscillation is more apparent, both in the longitudinal division between the positive and negative TIs and in the balance between high and low anomalies in the SLP field across the Mediterranean basin. These schemes coincide with similar results obtained by Maheras (1981), and Douguédroit (1993) reported about negative correlation between precipitation in the western and eastern Mediterranean. Similar results were also obtained for the temperature regime (Kutiel and Maheras, 1998).

Particularly in winter, but also to an extent in spring and autumn, the widespread distribution of high temperatures over the Mediterranean is associated with a negative SLP anomaly well to the west (in this case, the Mediterranean basin, which may be covered by a relatively high pressure field) that produces southwesterly flow from the ocean into the western Mediterranean, which may penetrate eastwards, or allow warmer air from North Africa to influence eastern parts of the basin. In contrast, particularly cold months occur in winter, when the flow is meridional, introducing a northerly component to the flow into the Mediterranean. Some of the most pronounced basin-wide cold events, in autumn as well as in winter, are associated with positive SLP anomalies, to the west or northwest of the British Isles, whilst lower-than-normal SLP is located southwards. This pressure distribution is associated with an extreme phase of the NAO, which is frequently related to low temperatures over large parts of the Mediterranean, as well as other areas in Europe (Moses *et al.*, 1987).

The results reported here confirm the conclusions of others (Reddaway and Bigg, 1996; Maheras *et al.*, 1997) that the prevailing temperature in the west–central Mediterranean is influenced by circulation over the Atlantic, whilst the eastern part of the basin is subject to varying influences, dependent on circulation over southern Asia, North Africa, east–central Europe, and on season.

It is anticipated that the relationships discussed here will be of use for the purposes of the reconstruction of circulation patterns at the monthly scale, and for earlier periods when it is possible to derive TIs based on a combination of instrumental and documentary observations, or even on documentary information alone (Kington, 1994; Wanner *et al.*, 1994; Grove and Conterio, 1995).

ACKNOWLEDGEMENTS

This research was funded by EC project ADVICE under contract ENV4-CT95-0129 (DG 12-ESCY). The authors greatly appreciate P. Jones for providing unpublished gridded pressure data, final version of ADVICE product.

REFERENCES

- Bartzokas, A. and Metaxas, D.A. 1991. 'Climatic fluctuations of temperature and air circulation in the Mediterranean', in Duplessy, J.C., Pons, A. and Fantechi, R. (eds), *Proceedings of the Course on Climate and Global Change of the European School of Climatology and Natural Hazards*, Arles, European Commission, Luxembourg, pp. 279–298.
- Besleaga, N. 1991. 'Vagues de froid sur la France et les pays voisins', in Phénomènes Remarquables No 2, SCEM, Paris, p. 41.
- Conte, M., Giuffrida, A. and Tedesco, S. 1989. 'The Mediterranean oscillation. Impact on precipitation and hydrology in Italy', in *Conference on Climate, Water*, Pub. of the Academy of Finland, Helsinki, pp. 121–137.
- Corte-Real, S., Zhang, X. and Wang, X. 1995. 'Large-scale circulation regimes and surface climatic anomalies over the Mediterranean', *Int. J. Climatol.*, **15**, 1135–1150.
- Douguédroit, A. 1993. 'A propos de la sécheresse dans le bassin Méditerranéen', *Pub. Assoc. Int. Climatol.*, **6**, 15–23.
- Giles, B.D. and Balafoutis, C.I. 1990. 'The Greek heatwaves of 1987 and 1998', *Int. J. Climatol.*, **10**, 505–517.
- Grove, J.M. and Conterio, A. 1995. 'The climate of Crete in the sixteenth and seventeenth centuries', *Clim. Change*, **30**, 223–247.
- Jones, P.D., Davies, T.D., Lister, D.H., Slonosky, V., Jónsson, T., Barring, L., Jonsson, P., Maheras, P., Kolyva-Machera, F., Barriendos, M., Martin-Vide, J., Alcoforado, M.J., Wanner, H., Pfister, C., Schuepbach, E., Kaas, E., Schmith, T., Jacobeit, J. and Beck, C. 1999. 'Monthly mean pressure reconstructions for Europe', *Int. J. Climatol.*, **19**, 347–364.
- Kaiser, H.F. 1959. 'Computer program for Varimax rotation in Factor Analysis', *Edu. Psycho. Meas.*, **19**, 413–420.
- Kington, J. 1994. 'Synoptic weather mapping, 1675–1715', in *Climatic Trends and Anomalies in Europe 1675–1715*, G. Fischer, Stuttgart, pp. 389–399.
- Kozukowski, K., Wibig, L. and Maheras, P. 1992. 'Connections between air temperature and the geopotential height of the 500 hPa level in a meridional cross-section in Europe', *Int. J. Climatol.*, **12**, 343–352.
- Kutiél, H., Maheras, P. and Guika, S. 1996. 'Circulation and extreme rainfall conditions in the eastern Mediterranean during the last century', *Int. J. Climatol.*, **16**, 73–92.
- Kutiél, H. and Maheras, P. 1998. 'Variations in temperature regime across the Mediterranean during the last century and their relationship with circulation indices', *Theor. Appl. Climatol.*, **61**, 39–53.
- Maheras, P. 1981. 'La variabilité des précipitations dans la mer Egée', *Arch. Met. Geophys. Biokl.*, **29B**, 157–166.
- Maheras, P. 1982. 'Climatologie de la mer Egée et de ses marges continentales. Etude de Climatologie descriptive et de Climatologie dynamique', in *Thèse d'Etat*, Atelier de Reproduction de thèses de Lille III, p. 787.
- Maheras, P. 1989. 'Principal component analysis of western Mediterranean air temperature variations, 1866–1985', *Theor. Appl. Climatol.*, **39**, 137–145.
- Maheras, P. and Kolyva-Machera, F. 1993. 'Variations spatiales et temporelles des précipitations saisonnières au-dessus des Balkans durant la dernière période séculaire', in *L'Eau, la Terre et les Hommes*, Hommage à R. Frécaut, PUN, pp. 163–172.
- Maheras, P., Kutiél, H. and Kolyva-Machera, F. 1997. 'Evolution de la pression atmosphérique en Europe méridionale et en Méditerranée durant la dernière période séculaire', *Publications de l'AIC*, **10**, 304–312.
- Maheras, P. and Kutiél, H. 1999. 'Spatial and temporal variations in the temperature regime in the Mediterranean and their relationship with circulation during the last century', *Int. J. Climatol.*, Accepted for publication.
- Metaxas, D.A. and Bartzokas, A. 1994. 'Pressure covariability over the Atlantic, Europe and N. Africa. Application: Centres of action for temperature, winter precipitations and summer winds in Athens, Greece', *Theor. Appl. Climatol.*, **49**, 9–18.
- Moses, T., Kiladis, G.N., Diaz, H.F. and Barry, R.G. 1987. 'Characteristics and frequency of reversals in mean sea level pressure in the North Atlantic sector and their relationship to long-term temperature trends', *J. Climatol.*, **7**, 13–30.
- Pfister, C., Kington, J., Kleinlogel, G., Schüle, H. and Siffert, E. 1994. 'High resolution spatio-temporal reconstructions of past climate from direct meteorological observations and proxy data', in *Climatic Trends and Anomalies in Europe 1675–1715*, G. Fischer, Stuttgart, pp. 329–375.
- Reddaway, J.M. and Bigg, G.R. 1996. 'Climatic change over the Mediterranean and links to more general atmospheric circulation', *Int. J. Climatol.*, **16**, 651–661.
- Richman, M. 1986. 'Rotation of principal components', *J. Climatol.*, **6**, 293–335.
- Rogers, J.C. 1984. 'The association between the North Atlantic Oscillation and the Southern Oscillation in the Northern Hemisphere', *Mon. Wea. Rev.*, **112**, 1999–2015.
- Rossetti, R. and Maheras, P. 1995. 'Variations pluviométriques durant la dernière période séculaire en Italie Septentrionale et Centrale', *Publications de l'AIC*, 327–336.
- Xoplaki, E., Maheras, P. and Luterbacher, J. 'Variability of climate in meridional Balkans during the period 1650–1850 and its impact on human life', in press.
- Wanner, H., Brázdil, R., Frich, P., Frydendahl, K., Jónsson, T., Kington, J., Pfister, C., Rosenørn, S. and Wishman, E. 1994. 'Synoptic interpretation of monthly weather maps for the Late Maunder Minimum (1675–1704)', in *Climatic Trends and Anomalies in Europe 1675–1715*, G. Fischer, Stuttgart, pp. 401–424.
- Wanner, H., Pfister, C., Brázdil, R., Frich, P., Frydendahl, K., Jónsson, T., Kington, J., Lamb, H.H., Rosenørn, S. and Wishman, E. 1995. 'Wintertime European circulation patterns during the Late Maunder Minimum cooling period (1675–1704)', *Theor. Appl. Climatol.*, **51**, 167–175.